Mobility matrix of a spherical particle translating and rotating in a viscous fluid confined in a spherical cell, and the rate of escape from the cell

B. U. Felderhof and A. Sellier

Citation: The Journal of Chemical Physics **136**, 054703 (2012); doi: 10.1063/1.3681368
View online: http://dx.doi.org/10.1063/1.3681368
View Table of Contents: http://scitation.aip.org/content/aip/journal/jcp/136/5?ver=pdfcov
Published by the AIP Publishing

Mobility matrix of a spherical particle translating and rotating in a viscous fluid confined in a spherical cell, and the rate of escape from the cell

B. U. Felderhof[1,a)] and A. Sellier[2,b)]
[1]*Institut für Theoretische Physik A, RWTH Aachen University, Templergraben 55, D-52056 Aachen, Germany*
[2]*LadHyx, École Polytechnique, 91128 Palaiseau Cédex, France*

(Received 14 November 2011; accepted 13 January 2012; published online 6 February 2012)

The mobility matrix of a spherical particle moving in a spherical cavity, filled with a viscous incompressible fluid, and with no-slip boundary condition at the wall of the cavity, is evaluated from the Oseen tensor for the cavity by the method used by Lorentz for a particle near a planar wall. For the case that the particle is a rigid sphere with no-slip boundary condition the comparison with exact calculations shows that the approximation is quite accurate, provided the radius of the particle is small relative to that of the cavity, and provided the particle is not too close to the wall. The translational mobility is used to derive the diffusion tensor of a Brownian particle via an Einstein relation. The approximate result for the diffusion tensor is employed to estimate the rate of escape of a Brownian particle from a cavity with semipermeable wall. © *2012 American Institute of Physics*. [doi:10.1063/1.3681368]

I. INTRODUCTION

Fluid flow on a small length scale is usually well described by low Reynolds number hydrodynamics. In the theoretical description, inertia is neglected and the fluid is assumed to be incompressible. The flow is dominated by shear viscosity. Flow velocity and pressure satisfy the steady state Stokes equations.[1,2]

A suspended particle moving in the fluid under the influence of an applied force causes a long range flow pattern, decaying at large distance in unbounded fluid only inversely with distance, as described by the well-known Oseen tensor. Hence, one expects that confinement in a vessel has a strong influence on the flow pattern and the mobility of the particle. The microrheology of a particle moving in a cavity is of great interest in technology, chemical physics, and biology.

In the following we consider a particle moving in a spherical cell, with fluid flow velocity satisfying the no-slip condition at the inner cell boundary. If the particle is a rigid sphere with no-slip boundary condition at its own surface, then the Stokes mobility functions for translation and rotation of the particle and the corresponding fluid flow pattern are completely known. The results are simple only when the particle is located at the center of the cavity.[1] The large amount of work for arbitrary distance from the wall has been summarized and corrected by Jones,[3] who also devised an efficient numerical scheme of computation. However, the exact solution of the problem is complicated and cumbersome. For practical purposes, it will be useful to have simple approximations to the mobility functions.

We derive an approximation to the mobility functions similar to that derived by Lorentz for a particle near a plane wall.[4] Lorentz started by deriving an expression for the Green function of the Stokes equations for a fluid bounded by a plane wall with no-slip boundary condition. The expression was later analyzed by Blake,[5] and cast in a different form by Kim and Karrila.[6] One can use the Green function to derive a first correction to the Stokes value for the mobility, by assuming the particle to be small in comparison with the distance to the wall. Lorentz' results for the translational mobility tensor, and similar ones derived for various geometries, have been summarized by Happel and Brenner.[7]

We use the Lorentz scheme for a spherical cell, employing the Green function derived by Oseen for a spherical cavity with no-slip boundary condition.[8,9] A comparison of the mobility functions with the exact results[3] shows that for a particle with radius one-tenth of the cell radius the approximation leads to surprisingly accurate results, except near the boundary. For the case of translational motion due to an applied force along a radius vector, we derive an improved approximation by taking account of a lubrication theory result for positions near the cell boundary.

The Lorentz scheme can also be used to derive an approximation to the mobility functions of a spherical particle of different structure, for example, a rigid particle with a mixed slip-stick boundary condition, a porous particle, or a droplet. This allows application to situations where no exact results are available. We expect that the approximate mobility functions are reasonably accurate.

We apply the derived translational mobility tensor to calculate the rate of escape from the cell for a diffusing particle with no-slip boundary condition at its surface. The position dependence of the diffusion tensor is found from the mobility tensor by means of an Einstein relation. We consider a spherically symmetric steady-state situation and show that confinement leads to a significantly reduced rate of escape, in comparison with a description with constant diffusion coefficient. The steady-state distribution is also strongly affected by the radial dependence of the translational mobility function.

a)Electronic mail: ufelder@physik.rwth-aachen.de.
b)Electronic mail: sellier@ladhyx.polytechnique.fr.

II. MOBILITY MATRIX

We consider a rigid spherical particle of radius a immersed in a viscous incompressible fluid contained in a motionless spherical cell of radius R. We use a Cartesian system of coordinates with the origin at the center of the cell. The particle is subjected to a force $\boldsymbol{F}$ and/or a torque $\boldsymbol{T}$. We assume that the resulting fluid flow satisfies the no-slip boundary condition at the inner surface S of the cell. For the time being, we assume also a no-slip boundary condition at the surface of the particle. In Sec. III, we shall extend the theory to a spherically symmetric particle with a more general boundary condition, to a porous particle, and to a droplet.

With neglect of inertia the flow velocity $\boldsymbol{v}$ and the pressure p satisfy the Stokes equations

$$\eta\nabla^2\boldsymbol{v} - \nabla p = 0, \quad \nabla\cdot\boldsymbol{v} = 0, \tag{2.1}$$

where η is the shear viscosity. As a consequence of the force $\boldsymbol{F}$ and the torque $\boldsymbol{T}$, the particle translates with velocity $\boldsymbol{U}$ and rotates with angular velocity $\boldsymbol{\Omega}$, given by the linear relation,

$$\begin{pmatrix} \boldsymbol{U} \\ \boldsymbol{\Omega} \end{pmatrix} = \begin{pmatrix} \boldsymbol{\mu}^{tt} & \boldsymbol{\mu}^{tr} \\ \boldsymbol{\mu}^{rt} & \boldsymbol{\mu}^{rr} \end{pmatrix} \begin{pmatrix} \boldsymbol{F} \\ \boldsymbol{T} \end{pmatrix}, \tag{2.2}$$

with a symmetric 6×6 mobility matrix $\boldsymbol{\mu}$, which depends on the position vector $\boldsymbol{r}_0$ of the particle center. By spherical symmetry we can decompose the mobility tensors $\boldsymbol{\mu}^{ab}$ in terms of scalar functions as

$$\begin{aligned} \mu^{tt}_{\rho\gamma} &= \alpha^{tt}(r_0)e_\rho e_\gamma + \beta^{tt}(r_0)(\delta_{\rho\gamma} - e_\rho e_\gamma), \\ \mu^{tr}_{\rho\gamma} &= \beta^{tr}(r_0)\varepsilon_{\rho\gamma\sigma}e_\sigma, \quad \mu^{rt}_{\rho\gamma} = \beta^{rt}(r_0)\varepsilon_{\rho\gamma\sigma}e_\sigma, \\ \mu^{rr}_{\rho\gamma} &= \alpha^{rr}(r_0)e_\rho e_\gamma + \beta^{rr}(r_0)(\delta_{\rho\gamma} - e_\rho e_\gamma), \end{aligned} \tag{2.3}$$

with radial unit vector $\boldsymbol{e} = \boldsymbol{r}_0/r_0$ and Levi-Civita tensor $\epsilon_{\rho\gamma\sigma}$. By symmetry $\beta^{rt} = -\beta^{tr}$. It is convenient to introduce dimensionless functions as

$$\begin{aligned} \tilde{\alpha}^{tt} &= 6\pi\eta a\alpha^{tt}, \quad \tilde{\beta}^{tt} = 6\pi\eta a\beta^{tt}, \\ \tilde{\beta}^{tr} &= 8\pi\eta a^2\beta^{tr}, \quad \tilde{\beta}^{rt} = 8\pi\eta a^2\beta^{rt}, \\ \tilde{\alpha}^{rr} &= 8\pi\eta a^3\alpha^{tt}, \quad \tilde{\beta}^{rr} = 8\pi\eta a^3\beta^{tt}. \end{aligned} \tag{2.4}$$

The so-called scalar mobility functions are known in explicit form from the solution of the flow problem in bipolar coordinates, see Ref. 3 and references cited there. However, the exact solution is quite complex. In this work, we aim rather at obtaining a simple approximation valid for $a \ll R$.

If only the force $\boldsymbol{F}$ is applied, then for $a \ll R$ and $|\boldsymbol{r} - \boldsymbol{r}_0| \gg a$, the solution of the flow Eq. (2.1), with $\boldsymbol{v} = 0$ at the inner surface of the cell, takes the form

$$\boldsymbol{v}(\boldsymbol{r},\boldsymbol{r}_0) = \mathsf{T}(\boldsymbol{r},\boldsymbol{r}_0)\cdot\boldsymbol{F}, \quad p(\boldsymbol{r},\boldsymbol{r}_0) = \boldsymbol{Q}(\boldsymbol{r},\boldsymbol{r}_0)\cdot\boldsymbol{F}, \tag{2.5}$$

with second-rank tensor field $\mathsf{T}(\boldsymbol{r},\boldsymbol{r}_0)$ and vector field $\boldsymbol{Q}(\boldsymbol{r},\boldsymbol{r}_0)$ independent of $\boldsymbol{F}$. These fields constitute the Green function solution of Eq. (2.1) for the geometry under consideration. In infinite space the Green function which tends to zero at infinity depends only on the vector distance $\boldsymbol{d} = \boldsymbol{r} - \boldsymbol{r}_0$ and takes the well-known Oseen form[1,2]

$$\mathsf{T}_0(\boldsymbol{r},\boldsymbol{r}_0) = \frac{1}{8\pi\eta}\frac{\mathsf{I}+\hat{\boldsymbol{d}}\hat{\boldsymbol{d}}}{d}, \quad \boldsymbol{Q}_0(\boldsymbol{r},\boldsymbol{r}_0) = \frac{1}{4\pi}\frac{\hat{\boldsymbol{d}}}{d^2}, \tag{2.6}$$

where I is the unit tensor and $\hat{\boldsymbol{d}} = \boldsymbol{d}/d$. We write the actual Green function as

$$\begin{aligned} \mathsf{T}(\boldsymbol{r},\boldsymbol{r}_0) &= \mathsf{T}_0(\boldsymbol{r},\boldsymbol{r}_0) + \mathsf{T}_R(\boldsymbol{r},\boldsymbol{r}_0), \\ \boldsymbol{Q}(\boldsymbol{r},\boldsymbol{r}_0) &= \boldsymbol{Q}_0(\boldsymbol{r},\boldsymbol{r}_0) + \boldsymbol{Q}_R(\boldsymbol{r},\boldsymbol{r}_0), \end{aligned} \tag{2.7}$$

where the reflection terms $\mathsf{T}_R(\boldsymbol{r},\boldsymbol{r}_0)$ and $\boldsymbol{Q}_R(\boldsymbol{r},\boldsymbol{r}_0)$ account for the reflected flow at the surface S. Thus, the tensor field $\mathsf{T}(\boldsymbol{r},\boldsymbol{r}_0)$ satisfies the no-slip boundary condition

$$\mathsf{T}(\boldsymbol{r},\boldsymbol{r}_0)\big|_{\boldsymbol{r}\in S} = 0, \qquad \boldsymbol{r}_0 \in V, \tag{2.8}$$

for any point $\boldsymbol{r}_0$ inside the cell volume V. The first terms T_0 and $\boldsymbol{Q}_0$ take care of the singular part of the Green function. The reflection terms T_R and $\boldsymbol{Q}_R$ are analytic in the components of $\boldsymbol{r}$ and $\boldsymbol{r}_0$ for $\boldsymbol{r} \in V$ and $\boldsymbol{r}_0 \in V$. The explicit expressions for the tensor $\mathsf{T}_R(\boldsymbol{r},\boldsymbol{r}_0)$ and the vector $\boldsymbol{Q}_R(\boldsymbol{r},\boldsymbol{r}_0)$ have been derived by Oseen,[8] and were later cast into an alternative form.[9]

We consider first the mobility tensor $\boldsymbol{\mu}^{tt}(\boldsymbol{r}_0)$. The approximate value is

$$\boldsymbol{\mu}^{tt}(\boldsymbol{r}_0) \approx \frac{1}{6\pi\eta a}\,\mathsf{I} + \mathsf{F}(\boldsymbol{r}_0), \tag{2.9}$$

where F is the reaction field tensor defined by[10]

$$\mathsf{F}(\boldsymbol{r}_0) = \mathsf{T}_R(\boldsymbol{r}_0,\boldsymbol{r}_0). \tag{2.10}$$

This takes account of the velocity of the lowest order reflected flow at the particle center. The correction term can be compared with that derived by Lorentz[4] for a plane wall. The contribution which would follow from Faxén's law[1] is omitted, since it would be proportional to a^2/R^2 and of the same order as that found from the reflection of the dipolar contribution to the Stokes flow of the particle. The Oseen tensor $\mathsf{T}_R(\boldsymbol{r}_0,\boldsymbol{r}_0)$ satisfies the reciprocity relation

$$\mathsf{T}_R(\boldsymbol{r},\boldsymbol{r}_0) = \tilde{\mathsf{T}}_R(\boldsymbol{r}_0,\boldsymbol{r}), \tag{2.11}$$

where the tilde indicates the transpose, so that the approximation (2.9) is compatible with the symmetry of the mobility tensor $\boldsymbol{\mu}^{tt}(\boldsymbol{r}_0)$.

In the same approximation the value of the tensor $\boldsymbol{\mu}^{rt}(\boldsymbol{r}_0)$ is found as

$$\boldsymbol{\mu}^{rt}(\boldsymbol{r}_0) \approx \frac{1}{2}((\nabla\times)(\mathsf{I})\mathsf{T}_R(\boldsymbol{r},\boldsymbol{r}_0))|_{\boldsymbol{r}=\boldsymbol{r}_0}, \tag{2.12}$$

where we have used a shorthand notation implying that the first factor $(\nabla\times)$ acts on the argument $\boldsymbol{r}$ and the first index of the tensor T_R, whereas the second factor (I) leaves the second index of the tensor T_R unchanged. The approximation takes account of the curl of the lowest order reflected flow at the particle center. Similarly, the tensor $\boldsymbol{\mu}^{tr}(\boldsymbol{r}_0)$ is found as

$$\boldsymbol{\mu}^{tr}(\boldsymbol{r}_0) \approx \frac{1}{2}((\mathsf{I})(\nabla_0\times)\mathsf{T}_R(\boldsymbol{r},\boldsymbol{r}_0))|_{\boldsymbol{r}=\boldsymbol{r}_0}, \tag{2.13}$$

where the second factor $(\nabla_0\times)$ acts on the argument $\boldsymbol{r}_0$ and the second index of the tensor T_R. The curl at the source point takes account of the action of a couplet.[11] It follows again by use of the reciprocity relation (2.11) that the expressions (2.12) and (2.13) are compatible with the symmetry of the mobility matrix.

Finally, we consider the tensor $\boldsymbol{\mu}^{rr}(\boldsymbol{r}_0)$. In the same approximation as above this is found as

$$\boldsymbol{\mu}^{rr}(\boldsymbol{r}_0) \approx \frac{1}{8\pi\eta a^3}\mathsf{I} + \frac{1}{4}((\nabla\times)(\nabla_0\times)\mathsf{T}_R(\boldsymbol{r},\boldsymbol{r}_0))|_{\boldsymbol{r}=\boldsymbol{r}_0}. \tag{2.14}$$

It follows from the reciprocity relation (2.11) that the approximate tensor is symmetric.

III. EXPLICIT EXPRESSIONS

In order to derive explicit expressions for the approximate mobility tensors, we use the explicit form of the reflection tensor $\mathsf{T}_R(\boldsymbol{r},\boldsymbol{r}_0)$ for the case of a spherical cavity with no-slip boundary condition, derived by Oseen.[8,9] His result reads

$$\begin{aligned}&\mathsf{T}_R(\boldsymbol{r},\boldsymbol{r}_0)\\ &= \frac{-1}{8\pi\eta}\Bigg[\frac{R}{r_0\overline{d}}\,\mathsf{I} + \frac{R^3}{r_0^3\overline{d}^{\,3}}(\boldsymbol{r}-\overline{\boldsymbol{r}_0})(\boldsymbol{r}-\overline{\boldsymbol{r}_0})\\ &\quad + \frac{r_0^2-R^2}{r_0}\Bigg(\frac{1}{R^3\overline{d}}\overline{\boldsymbol{r}_0}\,\overline{\boldsymbol{r}_0} - \frac{R}{r_0^2\overline{d}^{\,3}}\big(\overline{\boldsymbol{r}_0}(\boldsymbol{r}-\overline{\boldsymbol{r}_0})\\ &\quad + (\boldsymbol{r}-\overline{\boldsymbol{r}_0})\overline{\boldsymbol{r}_0}\big) - \frac{2}{R^3}\overline{\boldsymbol{r}_0}\,\overline{\boldsymbol{r}_0}\,\overline{\boldsymbol{r}_0}\cdot\nabla\frac{1}{\overline{d}}\Bigg) + (r^2-R^2)\nabla\boldsymbol{\phi}\Bigg],\end{aligned} \tag{3.1}$$

where the image point $\overline{\boldsymbol{r}_0}$ is defined by

$$\overline{\boldsymbol{r}_0} = \frac{R^2}{r_0^2}\boldsymbol{r}_0, \tag{3.2}$$

and $\overline{d}$ is the distance from the field point $\boldsymbol{r}$ to the image point

$$\overline{d} = |\boldsymbol{r}-\overline{\boldsymbol{r}_0}|. \tag{3.3}$$

Furthermore, with a slight simplification of Oseen's expression, the vector function $\boldsymbol{\phi}$ is given by

$$\begin{aligned}\boldsymbol{\phi}(\boldsymbol{r},\boldsymbol{r}_0) = \frac{r_0^2-R^2}{2r_0^3}\Bigg(&\frac{3}{Rr_0}\boldsymbol{r}_0 + \frac{R}{\overline{d}^{\,3}}(\boldsymbol{r}-\overline{\boldsymbol{r}_0}) + \frac{2}{R}\overline{\boldsymbol{r}_0}\,\overline{\boldsymbol{r}_0}\cdot\nabla\frac{1}{\overline{d}}\\ &+\frac{3r}{R\overline{d}}\frac{r-r_m}{r^2\overline{r_0}^2-(\boldsymbol{r}\cdot\overline{\boldsymbol{r}_0})^2}(R^2\boldsymbol{r}-\boldsymbol{r}\cdot\overline{\boldsymbol{r}_0}\,\overline{\boldsymbol{r}_0})\Bigg),\end{aligned} \tag{3.4}$$

with the abbreviation

$$r_m = (R^2 - r_0\overline{d})\frac{\boldsymbol{r}\cdot\boldsymbol{r}_0}{rr_0^2}. \tag{3.5}$$

The corresponding vector function $\boldsymbol{Q}_R(\boldsymbol{r},\boldsymbol{r}_0)$ is given by

$$\begin{aligned}&\boldsymbol{Q}_R(\boldsymbol{r},\boldsymbol{r}_0)\\ &= \frac{1}{4\pi}\Bigg[\Bigg(\frac{2}{d^3} - \frac{2R^3}{r_0^3\overline{d}^{\,3}}\Bigg)(\boldsymbol{r}-\overline{\boldsymbol{r}}_0) - 2\big(\boldsymbol{\phi} + 2\boldsymbol{r}\cdot\nabla\boldsymbol{\phi}\big)\Bigg].\end{aligned} \tag{3.6}$$

From the reflection tensor T_R, we find for the scalar functions defined in Sec. II

$$\tilde{\alpha}_1^{tt}(r) = 1 - \frac{9a}{4R}\frac{R^2}{R^2-r^2},$$

$$\tilde{\beta}_1^{tt}(r) = 1 - \frac{9a}{16R^3}\frac{4R^4-3R^2r^2+r^4}{R^2-r^2},$$

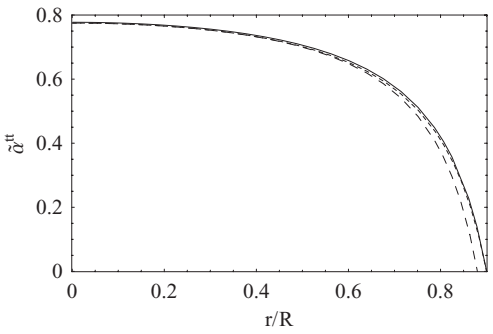

FIG. 1. Plot of $\tilde{\alpha}^{tt}(r)$ as a function of r/R for $a = 0.1\,R$, exact (solid) and approximate (long dashes). The exact function vanishes at $r = R - a$. We also plot the approximation $\tilde{\alpha}_2^{tt}(r)$, given by Eq. (4.12) (short dashes).

$$\begin{aligned}\tilde{\beta}_1^{tr}(r) &= \frac{3a^2r}{4R^3}\frac{2R^2-r^2}{R^2-r^2},\\ \tilde{\alpha}_1^{rr}(r) &= 1 - a^3\frac{R^3}{(R^2-r^2)^3},\\ \tilde{\beta}_1^{rr}(r) &= 1 - \frac{a^3}{4R^3}\frac{4R^6+12R^4r^2-9R^2r^4+3r^6}{(R^2-r^2)^3},\end{aligned} \tag{3.7}$$

where the subscript 1 is a reminder that this is only a first approximation. The functions are singular at $r = R$, but they are relevant only for $r < R - a$, since $R - a$ is the distance of closest approach. For $r = 0$, the expressions for $\tilde{\alpha}_1^{tt}(r)$ and $\tilde{\beta}_1^{tt}(r)$ reduce to $1 - (9a)/(4R)$ in agreement with Eq. (4-22.11) of Happel and Brenner[1] to first order in $\lambda = a/R$. The exact value is given by a ratio of two polynomials in λ of degree 5 and 4, respectively. For $r = 0$ the expressions for $\tilde{\alpha}_1^{rr}(r)$ and $\tilde{\beta}_1^{rr}(r)$ reduce to $1 - \lambda^3$ in agreement with Eq. (7-8.20) of Happel and Brenner.[1] This result is exact. The exact functions tend to zero as $r \to R - a$, except $\tilde{\alpha}^{rr}$. The approximate functions in Eq. (3.7) do not vanish at $r = R - a$.

The function $\tilde{\beta}_1^{tr}(r)$ vanishes at $r = 0$ and increases monotonically as r tends to $R - a$. A particle subject to a constant torque perpendicular to the radial direction will move on a circle in the plane of the torque and the radial unit vector. The translational velocity increases with r according to the approximate calculation. The calculation of Jones[3] shows that the exact function $\tilde{\beta}^{tr}(r)$ reaches a maximum at a value r_{max}, which depends on the ratio a/R. If $a < R/4$ the function reverses sign in the interval $r_{max} < r < R - a$, corresponding to a rolling motion near the spherical surface, and it tends to zero as $r \to R - a$. If $a > R/4$ there is no sign reversal. In Figs. 1–5, we show the approximate mobility functions as functions of r/R for $a/R = 0.1$, and compare with the exact ones. The agreement is quite good, except for r close to $R - a$.

It is clear from Eqs. (2.9)–(2.14) that the results derived above also yield approximate expressions for the scalar mobility functions of other types of spherical particle. We need to only replace Eq. (2.9) by

$$\boldsymbol{\mu}^{tt}(\boldsymbol{r}_0) \approx \mu_t\,\mathsf{I} + \mathsf{F}(\boldsymbol{r}_0), \tag{3.8}$$

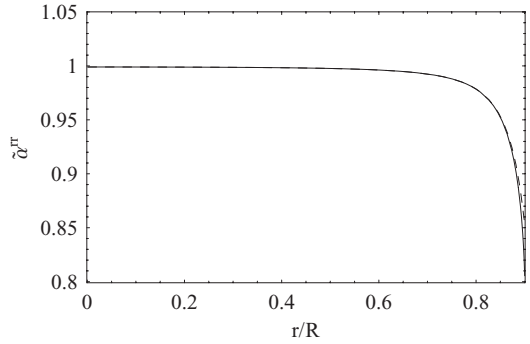

FIG. 2. Plot of $\tilde{\alpha}^{rr}(r)$ as a function of r/R for $a = 0.1\,R$, exact (solid) and approximate (dashed). The exact function is finite at $r = R - a$.

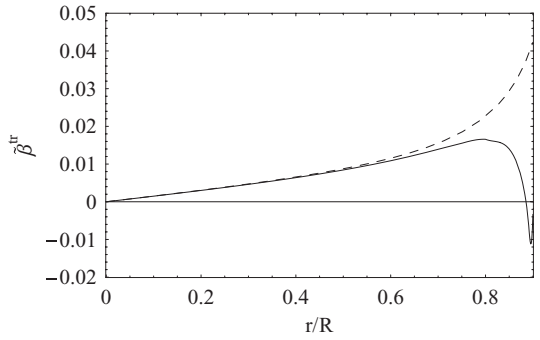

FIG. 4. Plot of $\tilde{\beta}^{tr}(r)$ as a function of r/R for $a = 0.1\,R$, exact (solid) and approximate (dashed). The exact function vanishes at $r = R - a$.

where μ_t is the translational mobility of the particle in infinite space. Similarly, Eq. (2.14) is replaced by

$$\boldsymbol{\mu}^{rr}(\boldsymbol{r}_0) \approx \mu_r\,\mathsf{I} + \frac{1}{4}\big((\nabla\times)(\nabla_0\times)\mathsf{T}_R(\boldsymbol{r},\boldsymbol{r}_0)\big)\big|_{\boldsymbol{r}=\boldsymbol{r}_0}, \quad (3.9)$$

where μ_r is the rotational mobility of the particle in infinite space. The explicit expressions are

$$\mu_t = \frac{1}{4\pi\eta A_{10}}, \quad \mu_r = \frac{1}{8\pi\eta A_{11}}, \quad (3.10)$$

where A_{10} and A_{11} are so-called hydrodynamic scattering coefficients. Explicit expressions have been derived for various examples of spherical particles, and have been summarized elsewhere.[12–14] The translational mobility tensor for a spherical particle can be expressed as

$$\boldsymbol{\mu}^{tt}(\boldsymbol{r}_0) = \mu_t\,\mathsf{I} - \frac{1}{6\pi\eta a}[(1-\tilde{\alpha}^{tt}(r_0))\hat{\boldsymbol{r}}_0\hat{\boldsymbol{r}}_0 + (1-\tilde{\beta}^{tt}(r_0))(\mathsf{I}-\hat{\boldsymbol{r}}_0\hat{\boldsymbol{r}}_0)], \quad (3.11)$$

where in our approximation the functions $\tilde{\alpha}^{tt}(r_0)$ and $\tilde{\beta}^{tt}(r_0)$ are replaced by $\tilde{\alpha}_1^{tt}(r_0)$ and $\tilde{\beta}_1^{tt}(r_0)$, as given by Eq. (3.7). Similarly, the rotational mobility tensor can be expressed as

$$\boldsymbol{\mu}^{rr}(\boldsymbol{r}_0) = \mu_r\,\mathsf{I} - \frac{1}{8\pi\eta a^3}[(1-\tilde{\alpha}^{rr}(r_0))\hat{\boldsymbol{r}}_0\hat{\boldsymbol{r}}_0 + (1-\tilde{\beta}^{rr}(r_0))(\mathsf{I}-\hat{\boldsymbol{r}}_0\hat{\boldsymbol{r}}_0)], \quad (3.12)$$

where in our approximation the functions $\tilde{\alpha}^{rr}(r_0)$ and $\tilde{\beta}^{rr}(r_0)$ are replaced by $\tilde{\alpha}_1^{rr}(r_0)$ and $\tilde{\beta}_1^{rr}(r_0)$, as given by Eq. (3.7). Note that in our approximation the second term in Eqs. (3.11) and (3.12) is independent of the particle radius a.

The coupling tensors $\boldsymbol{\mu}^{tr}$ and $\boldsymbol{\mu}^{rt}$ are given by Eqs. (2.3) and (2.4) with the scalar mobility function $\tilde{\beta}^{tr}(r_0)$ replaced in our approximation by $\tilde{\beta}_1^{tr}(r_0)$, as given by Eq. (3.7). Note that in our approximation the mobility tensors $\boldsymbol{\mu}^{tr}$ and $\boldsymbol{\mu}^{rt}$ are independent of the particle radius a and of the particle structure. A constant torque applied to the particle will cause circular orbital motion parallel to the wall of the cavity, with a period which depends only on the distance from the center. Near the wall the approximate mobility function differs rather strongly from the exact one, as shown in Fig. 4.

IV. ESCAPE FROM THE CELL

As an application we consider the situation where the cell wall is a semipermeable membrane through which the particle can escape. As a model we assume that the particle is created at the origin at a certain rate and then diffuses in the cell by thermal motion, as governed by the diffusion equation

$$\frac{\partial n}{\partial t} = \nabla\cdot\boldsymbol{D}(\boldsymbol{r})\cdot\nabla n, \quad 0 < r < R, \quad (4.1)$$

with number density n and diffusion tensor $\boldsymbol{D}$ given by the Einstein relation

$$\boldsymbol{D}(\boldsymbol{r}) = k_B T\,\boldsymbol{\mu}^{tt}(\boldsymbol{r}), \quad (4.2)$$

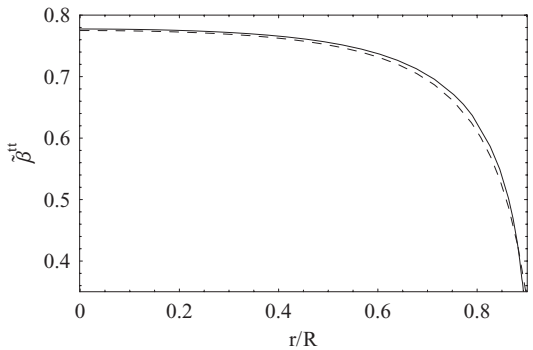

FIG. 3. Plot of $\tilde{\beta}^{tt}(r)$ as a function of r/R for $a = 0.1\,R$, exact (solid) and approximate (dashed). The exact function vanishes at $r = R - a$.

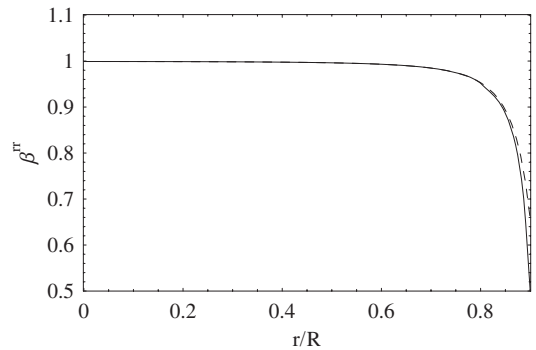

FIG. 5. Plot of $\tilde{\beta}^{rr}(r)$ as a function of r/R for $a = 0.1\,R$, exact (solid) and approximate (dashed). The exact function vanishes at $r = R - a$.

where k_B is Boltzmann's constant and T is absolute temperature. We assume that the particle is not subject to potential interactions inside the cell.

The particle can escape through pores in the cell membrane. It is assumed that these are distributed approximately uniformly on the surface of the cell, so that the latter may be taken to be isotropic. The escape is modeled by the boundary condition

$$\xi \frac{dn}{dr}|_{R_c} + n|_{R_c} = 0, \tag{4.3}$$

where ξ is an absorption length and R_c is the escape radius. The latter must be taken to be slightly less than the radius $R - a$ if the particle is modeled as a rigid sphere of radius a with no-slip boundary condition, for then the radial component of the translational mobility tensor behaves as[3]

$$\mu_{rr}^{tt}(\boldsymbol{r}) \approx \frac{1}{6\pi\eta a}\left(1 - \frac{a}{R}\right)^2\left(\frac{R-r}{a} - 1\right), \tag{4.4}$$

near the boundary. We must have $R - R_c > a$, otherwise the particle will never escape. The absorption length ξ and the escape radius R_c characterize the properties of the cell membrane.

We consider a steady-state process in which $n(\boldsymbol{r})$ satisfies

$$\nabla \cdot \boldsymbol{D}(\boldsymbol{r}) \cdot \nabla n = -Q\delta(\boldsymbol{r}), \tag{4.5}$$

where Q is the production rate. By symmetry the solution of Eq. (4.5) is radially symmetric, and can be integrated once to yield

$$D_{rr}(r)r^2\frac{dn}{dr} = -J, \quad 0 < r < R_c, \tag{4.6}$$

where the constant J is the flux.

For constant diffusion coefficient $D_0 = k_BT/6\pi\eta a$ the solution would be

$$n_0(r) = \frac{Q}{4\pi D_0}\left(\frac{1}{r} - \frac{1}{R_c} + \frac{\xi}{R_c^2}\right), \tag{4.7}$$

corresponding to current density

$$j_0(r) = \frac{Q}{4\pi r^2}, \tag{4.8}$$

and flux $J = Q/4\pi$. The number of particles passing per second through any spherical surface centered about the origin is Q. The number of particles in the sphere of radius R_c equals

$$N_0 = \int_{r<R_c} n_0\, d\boldsymbol{r} = \frac{Q}{6D_0}R_c(R_c + 2\xi). \tag{4.9}$$

Hence, the escape rate is

$$\gamma_0 = \frac{Q}{N_0} = \frac{6D_0}{R_c(R_c + 2\xi)}. \tag{4.10}$$

The approximate scalar function $\tilde{\alpha}_1^{tt}(r)$, given by Eq. (3.7), has the form

$$\tilde{\alpha}_1^{tt}(r) = \frac{b^2 - r^2}{R^2 - r^2}, \quad b = \sqrt{R^2 - \frac{9}{4}aR}. \tag{4.11}$$

This vanishes at $r = b$, rather than at $r = R - a$, as given by Eq. (4.4). We improve the approximate mobility as a function of r by slightly shifting the pole in Eq. (4.11). We require that the improved approximation $\tilde{\alpha}_2^{tt}(r)$ vanishes at $r = R - a$, has the value b^2/R^2 at $r = 0$, and the same coefficient of r^2 as $\tilde{\alpha}_1^{tt}(r)$ in an expansion in powers of r^2. These requirements yield

$$\tilde{\alpha}_2^{tt}(r) = 4\frac{b^4}{R}\,\frac{(R-a)^2 - r^2}{4b^2R(R-a)^2 - Cr^2}, \tag{4.12}$$

with coefficient

$$C = 4R^3 - 18aR^2 + 18a^2R - 9a^3. \tag{4.13}$$

In Fig. 1, we also plot the function $\tilde{\alpha}_2^{tt}(r)$ for $a = 0.1\,R$. This shows that the approximate values are quite accurate. A similar approximation does not work for the other hydrodynamic functions in Eq. (3.7).

With use of the approximate diffusion coefficient

$$D_{rr}(r) = D_0\tilde{\alpha}_2^{tt}(r), \tag{4.14}$$

the solution of Eq. (4.6) with $J = Q/4\pi$ is

$$n(r) = \frac{QR^2}{4\pi D_0 b^2}\left[\frac{1}{r} - \frac{A}{R_c} + B\log\frac{(R-a-r)(R-a+R_c)}{(R-a+r)(R-a-R_c)}\right], \tag{4.15}$$

with coefficient B given by

$$B = \frac{9a(R-a)}{8b^2R}. \tag{4.16}$$

The boundary condition (4.3) yields for the coefficient A

$$A = 1 - \frac{\xi}{R_c} - 2\xi\frac{(R-a)R_c}{(R-a)^2 - R_c^2}B. \tag{4.17}$$

From the integral

$$N = \int_{r<R_c} n\, d\boldsymbol{r}, \tag{4.18}$$

one finds the escape rate

$$\gamma = \frac{Q}{N} = D_0\frac{b^2}{R^2}\left[\left(\frac{1}{2} - \frac{1}{3}A\right)R_c^2 + \frac{1}{3}B\left((R-a)^3\log\frac{(R-a)^2}{(R-a)^2 - R_c^2} - (R-a)R_c^2\right)\right]^{-1}. \tag{4.19}$$

In Fig. 6, we plot the reduced radial density $r^2\tilde{n}(r) = 4\pi D_0 r^2 n(r)/Q$ as a function of r/R for $a = 0.1\,R$, $\xi = 0$, and $R_c = 0.89\,R$, and compare with $r^2\tilde{n}_0(r) = 4\pi D_0 r^2 n_0(r)/Q$. We define the reduced rate as

$$\tilde{\gamma} = R_c^2\gamma/(6D_0). \tag{4.20}$$

For the values corresponding to Fig. 6, the reduced rate is $\tilde{\gamma} = 0.461$ compared with $\tilde{\gamma}_0 = 1$. In Fig. 7, we plot the reduced radial density $r^2\tilde{n}(r) = 4\pi D_0 r^2 n(r)/Q$ as a function of r/R for $a = 0.1\,R$, $\xi = 2a$, and $R_c = 0.89\,R$, and compare with $r^2\tilde{n}_0(r) = 4\pi D_0 r^2 n_0(r)/Q$. For these values the reduced rate is $\tilde{\gamma} = 0.114$ compared with $\tilde{\gamma}_0 = 0.690$. In both cases the additional hydrodynamic friction has a strong effect on the distribution and on the rate of escape.

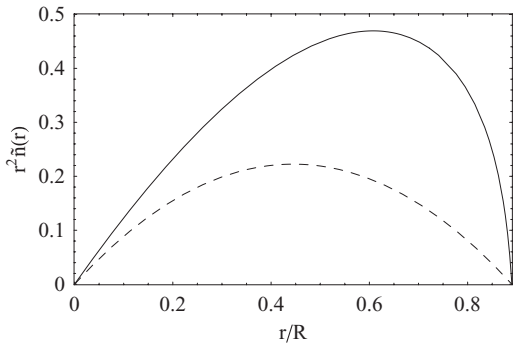

FIG. 6. Plot of the reduced radial density $r^2\tilde{n}(r) = 4\pi D_0 r^2 n(r)/Q$ as a function of r/R for $a = 0.1\,R$, $\xi = 0$, and $R_c = 0.89\,R$ (solid curve), compared with $r^2\tilde{n}_0(r) = 4\pi D_0 r^2 n_0(r)/Q$ (dashed curve).

V. DISCUSSION

We have found good agreement between approximate and exact results for the mobility functions of a spherical particle in a spherical cavity for the case where the particle is a rigid sphere with no-slip boundary condition.[3] This encourages one to use the approximation also for other types of spherical particle confined to a spherical cavity, as discussed at the end of Sec. III. The simplicity of the approximate mobility functions allows easy application, as we have shown in Sec. IV in the calculation of the rate of escape of a Brownian particle from the cell.

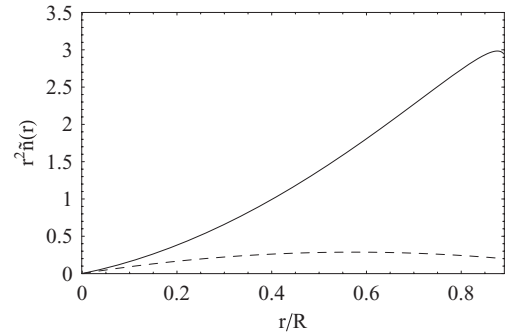

FIG. 7. Plot of the reduced radial density $r^2\tilde{n}(r) = 4\pi D_0 r^2 n(r)/Q$ as a function of r/R for $a = 0.1\,R$, $\xi = 0.2\,a$, and $R_c = 0.89\,R$ (solid curve), compared with $r^2\tilde{n}_0(r) = 4\pi D_0 r^2 n_0(r)/Q$ (dashed curve).

Restricted diffusion is a common feature of many physicochemical, biological, and industrial processes. Our calculation shows that the hydrodynamic interaction with the wall of the cavity has a strong influence on steady-state diffusion. It will be of interest to study also the effect on the dynamics of Brownian motion of the confined particle. This requires a discussion of the time-dependent diffusion process in the confined space.[15]

The approximate translational-rotational mobility tensor is particularly simple. As discussed at the end of Sec. III, it is independent of the structure of the spherical particle, and of its radius. In the approximation, a constant torque applied to the particle will cause circular orbital motion parallel to the wall of the cavity, with a period which depends only on the distance from the center. For the case where the particle is a sphere with no-slip boundary condition the exact motion has been studied by Jones.[3] It follows from the exact calculation that for fixed torque the particle reverses direction if the orbit is close to the wall. This curious effect is missed in the approximate calculation.

[1]J. Happel and H. Brenner, *Low Reynolds Number Hydrodynamics* (Noordhoff, Leyden, 1973).
[2]S. Kim and S. J. Karrila, *Microhydrodynamics* (Butterworth-Heinemann, Stoneham, Massachusetts, 1991).
[3]R. B. Jones, in *Theoretical Methods for Microscale Viscous Flows*, edited by F. Feuillebois and A. Sellier (Transworld Research Network, Kerala, India, 2009), p. 61.
[4]H. A. Lorentz, Abh. Theor. Physik **1**, 23 (1907).
[5]J. R. Blake, Proc. Cambridge Philos. Soc. **70**, 303 (1971).
[6]S. Kim and S. J. Karrila, *Microhydrodynamics* (Butterworth-Heinemann, Stoneham, Massachusetts, 1991), Chap. 12. Note that the first term on the right side of Eq. (12.1) must have a plus sign, rather than a minus sign.
[7]J. Happel and H. Brenner, *Low Reynolds Number Hydrodynamics* (Noordhoff, Leyden, 1973), p. 341.
[8]C. W. Oseen, *Hydrodynamik* (Akademische Verlagsgesellschaft, Leipzig, 1927).
[9]A. Sellier, Comput. Model. Eng. Sci. **25**, 165 (2008).
[10]B. U. Felderhof, J. Phys. Chem. B **109**, 21406 (2005).
[11]G. K. Batchelor, J. Fluid Mech. **41**, 545 (1970).
[12]B. Cichocki, B. U. Felderhof, and R. Schmitz, PhysicoChem. Hydrodyn. **10**, 383 (1988).
[13]B. U. Felderhof, J. Chem. Phys. **125**, 124904 (2006).
[14]B. Cichocki and B. U. Felderhof, J. Chem. Phys. **130**, 164712 (2009).
[15]D. S. Grebenkov, Rev. Mod. Phys. **79**, 1077 (2007).